

2004

Exploration of Artificial Multiferroic Thin-Film Heterostructures using Composition Spreads

K.-S. Chang

M. A. Aronova

C.-L. Lin

M. Murakami

M.-H. Yu

See next page for additional authors

Follow this and additional works at: https://scholarcommons.sc.edu/eche_facpub



Part of the [Chemical Engineering Commons](#), [Electromagnetics and Photonics Commons](#), and the [Other Materials Science and Engineering Commons](#)

Publication Info

Published in *Applied Physics Letters*, Volume 84, Issue 16, 2004, pages #3091-.

This Article is brought to you by the Chemical Engineering, Department of at Scholar Commons. It has been accepted for inclusion in Faculty Publications by an authorized administrator of Scholar Commons. For more information, please contact digres@mailbox.sc.edu.

Author(s)

K.-S. Chang, M. A. Aronova, C.-L. Lin, M. Murakami, M.-H. Yu, Jason R. Hattrick-Simpers, O. O. Famodu, S. Y. Lee, R. Ramesh, M. Wuttig, I. Takeuchi, C. Gao, and L. A. Bendersky

Exploration of artificial multiferroic thin-film heterostructures using composition spreads

K.-S. Chang, M. A. Aronova, C.-L. Lin, M. Murakami, M.-H. Yu, J. Hattrick-Simpers, O. O. Famodu, S. Y. Lee, R. Ramesh, M. Wuttig, I. Takeuchi, C. Gao, and L. A. Bendersky

Citation: *Applied Physics Letters* **84**, 3091 (2004); doi: 10.1063/1.1699474

View online: <http://dx.doi.org/10.1063/1.1699474>

View Table of Contents: <http://scitation.aip.org/content/aip/journal/apl/84/16?ver=pdfcov>

Published by the AIP Publishing

Articles you may be interested in

[Room temperature magnetoelectric coupling in \$\text{Zn}_{1-x}\text{Co}_x\text{O}/\text{BaTiO}_3\$ bilayer system](#)

Appl. Phys. Lett. **105**, 132902 (2014); 10.1063/1.4896771

[Significant enhancement of magnetoelectric output in multiferroic heterostructural films modulated by electric polarization cycles](#)

Appl. Phys. Lett. **96**, 152902 (2010); 10.1063/1.3394008

[Influence of relative thickness on multiferroic properties of bilayered \$\text{Pb}\(\text{Zr}_{0.52}\text{Ti}_{0.48}\)\text{O}_3 - \text{CoFe}_2\text{O}_4\$ thin films](#)

J. Appl. Phys. **104**, 114114 (2008); 10.1063/1.3035851

[Strong magnetoelectric coupling in \$\text{Tb} - \text{Fe}/\text{Pb}\(\text{Zr}_{0.52}\text{Ti}_{0.48}\)\text{O}_3\$ thin-film heterostructure prepared by low energy cluster beam deposition](#)

Appl. Phys. Lett. **92**, 012920 (2008); 10.1063/1.2831695

[Magnetoelectric \$\text{CoFe}_2\text{O}_4 - \text{Pb}\(\text{Zr}, \text{Ti}\)\text{O}_3\$ composite thin films derived by a sol-gel process](#)

Appl. Phys. Lett. **86**, 122501 (2005); 10.1063/1.1889237

The advertisement features a photograph of the Model PS-100 cryogenic probe station, which is a complex piece of scientific equipment with various mechanical components and a probe. The background is a gradient of blue. On the left, the text 'Model PS-100' is in a large, bold, white font, with 'Tabletop Cryogenic Probe Station' in a smaller white font below it. On the right, the 'Lake Shore CRYOTRONICS' logo is displayed, with 'Lake Shore' in a large, white, serif font and 'CRYOTRONICS' in a smaller, white, sans-serif font below it. Below the logo, the tagline 'An affordable solution for a wide range of research' is written in a white, italicized, serif font.

Exploration of artificial multiferroic thin-film heterostructures using composition spreads

K.-S. Chang, M. A. Aronova,^{a)} C.-L. Lin, M. Murakami, M.-H. Yu, J. Hattrick-Simpers, O. O. Famodu, S. Y. Lee,^{a)} R. Ramesh,^{a)} M. Wuttig, and I. Takeuchi^{a),b)}
Small Smart Systems Center, Department of Materials Science and Engineering, University of Maryland, College Park, Maryland 20742

C. Gao

National Synchrotron Radiation Laboratory, University of Science and Technology of China, Hefei, Anhui, China 230029

L. A. Bendersky

NIST, Gaithersburg, Maryland 20899

(Received 19 November 2003; accepted 10 February 2004)

We have fabricated a series of composition spreads consisting of ferroelectric BaTiO_3 and piezomagnetic CoFe_2O_4 layers of varying thicknesses modulated at nanometer level in order to explore artificial magnetoelectric thin-film heterostructures. Scanning microwave microscopy and scanning superconducting quantum interference device microscopy were used to map the dielectric and magnetic properties as a function of continuously changing average composition across the spreads, respectively. Compositions in the middle of the spreads were found to exhibit ferromagnetism while displaying a dielectric constant as high as ≈ 120 . © 2004 American Institute of Physics. [DOI: 10.1063/1.1699474]

Magnetoelectric materials¹ are one class of multiferroics in which charge polarization and magnetization coexist and are coupled together. Such materials can display a magnetoelectric effect in which change in magnetization is induced by an electric field and change in electric polarization is induced by an applied magnetic field. This property can be used as a basis for novel actuators and sensors with high sensitivity.² Van Suchtelen and co-workers^{3–5} made the first artificial magnetoelectric material by combining a ferroelectric (piezoelectric) material BaTiO_3 (BTO) and a ferromagnetic (piezomagnetic) material CoFe_2O_4 (CFO) in an eutectic sintered composite. There have also been reports of magnetoelectric effects in layered composites such as $(\text{Pb,Zr})\text{TiO}_3$ (PZT)– $\text{Tb}_{0.3}\text{Dy}_{0.7}\text{Fe}_{1.92}$ (Terfenol-D), PZT– NiFeO_4 , polyvinylidene fluoride–Terfenol-D and laminate $\text{Pb}(\text{Mg}_{1/3}\text{Nb}_{2/3})\text{O}_3$ – PbTiO_3 –Terfenol-D.^{6–9}

To date, these composite materials have been exclusively studied in bulk materials. The present work explores the possibility of fabricating such materials in a thin-film form. Thin-film samples have several advantages over bulk samples: (1) magnetoelectric thin-film heterostructures can be constructed by alternating piezoelectric and piezomagnetic layers, and one can investigate coupling of the two properties at nanometer levels; and (2) one can pursue fabrication of compact thin-film magnetoelectric devices. Our initial goal is to create materials that are simultaneously ferroelectric and ferromagnetic. We explore this by fabricating structures in which ferroelectric and ferromagnetic layers alternate with nanometer-thick periods. In constructing such structures, there are many parameters to be optimized: compositions, thickness of each layer, etc. In order to rapidly

map the parameter space, we implement the continuous composition spread approach. In particular, we use a design of the spread in which one end of the spread is a pure piezoelectric material and the other end is a pure piezomagnetic material, and they are gradually mixed together toward the center of the spread. This technique allows us to systematically investigate mixing and changing of the two physical properties as a function of average composition, which continuously varies across the spread (Fig. 1). The magnetoelectric coefficient has been reported to be a function of the ratio of the volume of the piezoelectric phase to the volume of the piezomagnetic phase in bilayered or multilayered structures.^{10–12} The present composition spread technique can offer an efficient way to systematically optimize the volume ratio to obtain the maximum magnetoelectric effect. Here, BTO and CFO are used as the ferroelectric and ferromagnetic materials, respectively.

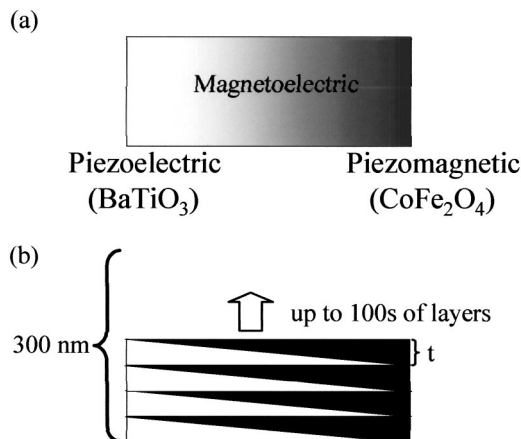


FIG. 1. (a) The schematic of the composition spreads. (b) Synthesis scheme of the spread. The thickness of each wedge can be varied from less than one unit cell to multiples of unit cells at the thick end. The total thickness is 300 nm everywhere.

^{a)}Also at: Center for Superconductivity Research, Department of Physics, University of Maryland, College Park, MD 20742.

^{b)}Electronic mail: takeuchi@squid.umd.edu

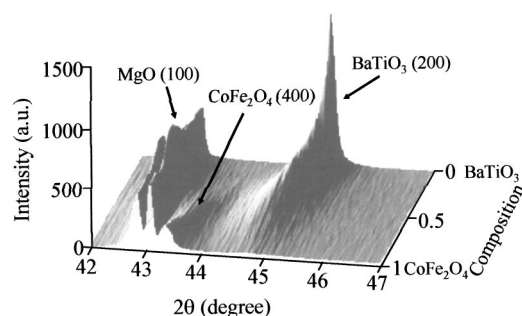


FIG. 2. The scanning x-ray microdiffraction of the spread sample, for which t is 1.68 nm. The intensity is plotted as a function of 2θ (from 42° to 47°) and as a function of average composition (from pure BTO to pure CFO).

Previously, we have fabricated high-quality composition spreads of $(\text{Ba}_x\text{Sr}_{1-x})\text{TiO}_3$.¹³ Unlike these previous studies, BTO and CFO do not form solid solutions, and thus, in order to provide some “integrity” in the respective materials, spreads were made in such a way that there is more than one unit cell of BTO and CFO at the thick end of each wedge layer (henceforth defined as t). We made a series of composition spreads in which t was approximately 0.84, 2.52, 8.4, and 12.6 nm [see Fig. 1(b)]. These numbers roughly correspond to $1\times$, $3\times$, $10\times$, and $15\times$ the unit cell of CFO. BTO has a pseudocubic structure with the lattice constant $a=0.403$ nm, and CFO has a spinel cubic structure with the lattice constant $a=0.839$ nm. Although the two materials have different structures, the mismatch between twice the lattice parameter of BTO and that of CFO is roughly 5%, and we have found that they can be grown together in a heteroepitaxial manner on (100) MgO (cubic with $a=0.42$ nm). The oxygen partial pressure during the deposition was 65 mTorr, and the substrate was held at the temperature of 800°C . The typical size and the thickness of a composition spread sample was 6 mm (in the spread direction) \times 10 mm and 300 nm (uniform across spreads), respectively. In each spread, the average composition continuously changes from pure BTO to pure CFO.

Structural changes of the BTO–CFO artificial multilayers across the spreads were studied by the ω -scan mode of a scanning x-ray microdiffractometer (D8 DISCOVER with GADDS for combinatorial screening by Bruker-AXS). A $300\text{ }\mu\text{m}$ spot size was used to take 20 points across each spread. The x-ray intensity as a function of 2θ and of the average composition for a spread in the 2θ range of 42° to 47° is shown in Fig. 2. The peaks are integrated from $-94.9^\circ < \chi < -78.4^\circ$. t was approximately 1.7 nm for this sample. It is seen that the (200) BTO peak and the (400) CFO peak continuously “evolve” toward the middle of the spread. The continuous shifts and the broadening of the peaks are indicative of significant and progressive lattice distortion caused by diffusion of cations (Ba^{2+} and Ti^{4+} of BTO and Co^{2+} and Fe^{3+} of CFO) at the multilayer interfaces. We have found that there is less lattice distortion toward the middle of the spread for spreads with larger thickness of the wedge layers; the x-ray peak positions do not shift in the middle of the spread for samples in which t is $10\times$ and $15\times$ the unit cell of CFO. This is consistent with the fact that in comparing spreads with different wedge thicknesses, there are fewer interfaces when the individual layer is thicker, and thus there

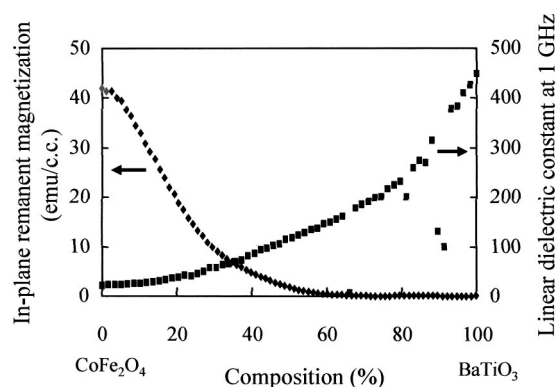


FIG. 3. Dielectric constant (right) measured by the microwave microscope, and the in-plane remanent magnetization (left), characterized by the scanning SQUID microscope as a function of average composition across the spread. t for this spread is 8.4 nm.

is a smaller overall fraction of materials affected by the interdiffusion at the interfaces.

In order to study the continuously changing properties of the spreads, microwave microscopy¹³ and room-temperature scanning superconducting quantum interference device (SQUID) microscopy were used. The linear dielectric constant measured at 1 GHz using the microwave microscope is shown in Fig. 3 for a spread in which t was 8.4 nm. The linear dielectric constant systematically decreases from 450 for the pure BTO end to 40 for the pure CFO end. The decreasing trend across the spread was found to be similar for all spreads, and the general trend is consistent with the one obtained from calculating the effective dielectric constant using the series capacitance model, in which layers with different dielectric constants are alternating. Comparing different spreads, we found that the dielectric constant at the same average composition is higher for the spreads with thicker wedge layers, consistent with the fact that thicker individual layers would have better overall materials integrity, as discussed earlier. This trend is evident in Fig. 4 for a dielectric constant measured at the average composition of $(\text{BTO})_{0.45}-(\text{CFO})_{0.55}$ for spreads with different wedge layer thicknesses. This trend may also be related to the ferroelectric size effect in thin films.^{14,15} The dielectric loss value at 1 GHz was found to vary continuously from ≈ 0.2 for the BTO end to ≈ 0.3 for the CFO end for all the spreads. These loss values are comparable to values obtained by other measure-

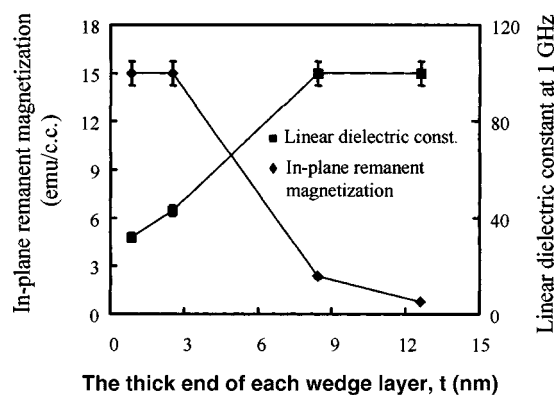


FIG. 4. Dielectric constant (right) and in-plane remanent magnetization (left) at the average composition $(\text{BTO})_{0.45}-(\text{CFO})_{0.55}$ from a series of composition spreads.

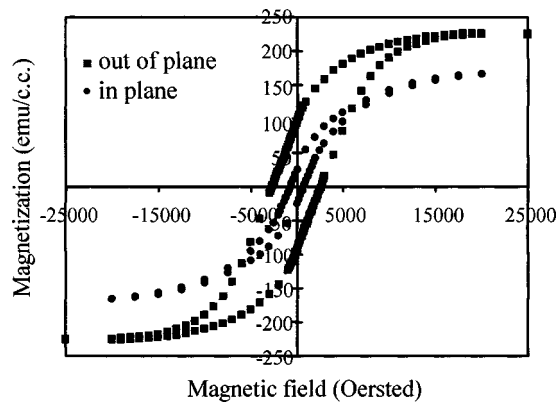


FIG. 5. A SQUID magnetometer measurement of M - H curves of a single composition sample of $(\text{BTO})_{0.45}\text{--}(\text{CFO})_{0.55}$. The periods of CFO and BTO layers are ≈ 1.4 nm and ≈ 1.1 nm, respectively.

ment methods for epitaxial $(\text{Ba,Sr})\text{TiO}_3$ films at microwave frequencies.^{16,17}

In order to characterize the ferromagnetic properties, mapping of magnetic field emanating from the sample due to remanent magnetization is obtained using a room-temperature scanning SQUID microscope. We magnetize our samples in the in-plane direction, even though the films studied here predominately showed the out-of-plane direction as the easy axis. This is because our present algorithm¹⁸ for obtaining quantitative remanent magnetization uses an in-plane magnetized model. The trend of how the in-plane remanent magnetization changes as a function of various parameters is used as an indicator of the overall magnetic properties. Comparing the in-plane remanent magnetization of the series of composition spreads at the same average composition, the spreads with thinner layer thicknesses seem to sustain higher remanent magnetization (as seen in Fig. 4). This could be explained by the mismatch stresses or strains between ferrite films and substrates, inducing enhanced magnetization for thinner layers.^{19,20} Despite the decaying of properties as one goes toward the middle of the spread, we see that there is a region that is magnetic and that has a reasonably high dielectric constant [≈ 120 at $(\text{BTO})_{0.5}\text{--}(\text{CFO})_{0.5}$]. High values of dielectric constant are often a good indicator of the presence of ferroelectricity.

The opposing thickness effect trend seen in Fig. 4 for magnetic and dielectric properties suggests that there is a compromise in obtaining both a high linear dielectric constant and high magnetization.

In order to confirm the dielectric and ferromagnetic properties observed here, a single composition sample with a uniform average composition of $(\text{BTO})_{0.45}\text{--}(\text{CFO})_{0.55}$, for which the periods of CFO and BTO layers were ≈ 1.4 nm and ≈ 1.1 nm, respectively, was fabricated. The dielectric constant of this sample was found to be ≈ 30 . Figure 5 shows the SQUID magnetometer measurement result, indicating the presence of ferromagnetism in this sample.

Initial transmission electron microscopy study of the spreads indicates that when the thickness of individual layer

is very thin (1–2 nm), the extent of the diffusion of BTO and CFO is such that eutectic separation seems to take place, leading to formation of separated nanoregions of BTO and CFO.²¹ This effect is expected to be less pronounced for structures with thicker individual layers (≥ 8 nm) in which the layered structures are expected to be maintained, in accord with the fact that no change in lattice constants was seen in the middle of the spreads for thicker individual wedge-layered samples. Further microstructural investigation and measurements to directly confirm the presence of ferroelectricity as well as the magnetoelectric effect using capacitors are currently underway.

The authors acknowledge A. Orozco and L. Knauss of Neocera, Inc. for assistance with the scanning SQUID measurement, and F. C. Wellstood and S. E. Lofland for valuable discussions. This project was funded by ONR N000140110761, NSF DMR 0094265 (CAREER), NSF DMR 0231291, MRSEC DMR-00-80008, DARPA DAAD19-03-1-0038, NSFC (50125207 and 60171044) and MOE (20010758025).

- ¹L. D. Landau and E. M. Lifshitz, *Electrodynamics of Continuous Media* (Gostekhizdat, Moscow, 1957).
- ²G. R. Slemmon, *Magnetoelectric Devices Transducers, Transformers, and Machines* (Wiley, New York, 1966).
- ³J. Van Den Boomgaard, A. M. J. G. Van Run, and J. Van Suchtelen, *Ferroelectrics* **14**, 727 (1976).
- ⁴J. Van Den Boomgaard, A. M. J. G. Van Run, and J. Van Suchtelen, *Ferroelectrics* **10**, 295 (1976).
- ⁵J. Van Suchtelen, *Philips Res. Rep.* **27**, 28 (1972).
- ⁶J. Ryu, A. V. Carazo, K. Uchino, and H.-E. Kim, *Jpn. J. Appl. Phys.* **40**, 4948 (2001).
- ⁷G. Srinivasan, E. T. Rasmussen, J. Gallegos, R. Srinivasan, Y. I. Bokhan, and V. M. Laletin, *Phys. Rev. B* **64**, 214408-1 (2001).
- ⁸K. Mori and M. Wuttig, *Appl. Phys. Lett.* **81**, 100 (2002).
- ⁹S. Dong, J.-F. Li, and D. Viehland, *Appl. Phys. Lett.* **83**, 2265 (2003).
- ¹⁰G. Harshé, J. P. Dougherty, and R. E. Newnham, *Int. J. Appl. Electro-magn. Mater.* **4**, 145 (1993).
- ¹¹G. Harshé, J. P. Dougherty, and R. E. Newnham, *Int. J. Appl. Electro-magn. Mater.* **4**, 161 (1993).
- ¹²M. Avellaneda and G. Harshé, *J. Intell. Mater. Syst. Struct.* **5**, 501 (1994).
- ¹³K.-S. Chang, M. Aronova, O. Famodu, I. Takeuchi, S. E. Lofland, J. Hattrick-Simpers, and H. Chang, *Appl. Phys. Lett.* **79**, 4411 (2001).
- ¹⁴T. M. Shaw, S. Trolier-McKinstry, and P. C. McIntyre, *Annu. Rev. Mater. Sci.* **30**, 263 (2000).
- ¹⁵H. Z. Jin and J. Zhu, *J. Appl. Phys.* **92**, 4594 (2002).
- ¹⁶Y. G. Wang, M. E. Reeves, W. J. Kim, J. S. Horwitz, and F. J. Rachford, *Appl. Phys. Lett.* **78**, 3872 (2001).
- ¹⁷J. C. Booth, L. R. Vale, and R. H. Ono, in *Materials Issues for Tunable RF and Microwave Devices*, edited by Q. X. Jia, F. A. Miranda, D. E. Oates, and X. X. Xi (Materials Research Society, Warrendale, PA, 2000), Vol. 606, pp. 253–264.
- ¹⁸E. F. Fleet, Ph.D. thesis, University of Maryland, College Park, 2000.
- ¹⁹J. Wang, J. B. Neaton, H. Zheng, V. Nagarajan, S. B. Ogale, B. Liu, D. Viehland, V. Vaithyanathan, D. G. Schlom, U. V. Waghmare, N. A. Spaldin, K. M. Rabe, M. Wuttig, and R. Ramesh, *Science* **299**, 1719 (2003).
- ²⁰G. Hu, J. H. Choi, C. B. Eom, V. G. Harris, and Y. Suzuki, *Phys. Rev. B* **62**, R779 (2000).
- ²¹H. Zheng, J. Wang, S. E. Lofland, Z. Ma, L. Mohaddes-Ardabili, T. Zhao, L. Salamana-Riba, S. R. Shinde, S. B. Ogale, F. Bai, D. Viehland, Y. Jia, D. G. Schlom, M. Wuttig, A. Roytburd, and R. Ramesh, *Science* **303**, 661 (2004).